

## Signal analysis of gravitational wave tails

This article has been downloaded from IOPscience. Please scroll down to see the full text article.

1994 Class. Quantum Grav. 11 2807

(<http://iopscience.iop.org/0264-9381/11/11/020>)

View [the table of contents for this issue](#), or go to the [journal homepage](#) for more

Download details:

IP Address: 134.157.250.66

The article was downloaded on 02/09/2011 at 17:52

Please note that [terms and conditions apply](#).

# Signal analysis of gravitational wave tails

Luc Blanchet† and B S Sathyaprakash‡

† Département d’Astrophysique Relativiste et de Cosmologie, Centre National de la Recherche Scientifique (UPR 176), Observatoire de Paris, 92 195 Meudon Cedex, France

‡ Inter-University Centre for Astronomy and Astrophysics, Post Bag 4, Ganeshkhind, Pune 411 007, India

Received 10 January 1994, in final form 16 June 1994

**Abstract.** The tails of gravitational waves result from the non-linear interaction between the usual quadrupole radiation generated by an isolated system (with total mass-energy  $M$ ), and the static monopole field associated with  $M$ . Their contributions to the field at large distances from the system include a particular effect of modulation of the phase in the Fourier domain, having  $M$  as a factor and depending on the frequency as  $\sim \omega \ln \omega$ . In this paper we investigate the level at which this tail effect could be detected in future laser interferometric detectors. We consider a family of matched filters of inspiralling compact binary signals, allowing for this effect and parametrized by a family of independent ‘test’ parameters including  $M$ . Detecting the effect is equivalent to attributing, by optimal signal processing, a non-zero value to  $M$ . The  $1 - \sigma$  error bar in the measurement of  $M$  is computed by analytical and numerical methods as a function of the optimal signal-to-noise ratio (SNR). We find that the minimal values of the SNR for detection of the tail effect at the  $1 - \sigma$  level range from  $\sim 100$  to  $\sim 2800$  for neutron-star binaries (depending on the type of noise in the detector and on our *a priori* knowledge of the binary), and from  $\sim 15$  to  $\sim 400$  for a black-hole binary with  $M = 20M_{\odot}$ . It is argued that some of these values, at least for black-hole binaries, could be achieved in future generations of detectors, following the currently planned VIRGO and LIGO detectors.

PACS numbers: 0430, 0480

## 1. Introduction

The late inspiral and final coalescence stages of compact (neutron-star or black-hole) binary systems should be routinely observed by future broadband gravitational wave detectors (see [1, 2] for reviews). The estimated number of final coalescence events of neutron stars is a few per year out to a distance of 100 Mpc [3–5]. At 100 Mpc, the first generation of VIRGO and LIGO detectors [6, 7] might observe the waves with a signal-to-noise ratio (SNR) of order 10 (see, for example, [8]); and future ‘advanced detectors’ could achieve very large SNRs indeed (see [9] for a discussion).

Optimal signal processing will be used in order to extract the useful gravitational signal out of the detector noise. This means that the raw output of the detector will be correlated with a family of matched (or Wiener) filters. A matched filter is a filter whose Fourier transform is equal to that of the signal divided by the power spectral density of the noise. A family of filters is required to deal with the unknown parameters of the signal, for instance, the two masses of the binary. Each filter in the family corresponds to a particular set of ‘test’ parameters, and by maximization of the correlation over these parameters, one identifies some ‘measured’ parameters, whose expectation values are equal to the parameters of the signal (for high enough SNR). This technique requires both that the spectral density

of the noise in the detector is measured, and that the form of the expected signal is known. In particular, the accuracy with which the signal is known determines the accuracy of the measurement of the parameters. It is now recognized [10] that taking higher-order (post-Newtonian) theoretical corrections into account in the construction of matched filters will be very important for an accurate measurement of the parameters. This is interesting because one will be able, as we shall see, to *detect* higher-order effects predicted by general relativity.

In this paper (which is a continuation of a previous paper [11]), we shall be interested in the detection of a particular *tail* effect, namely the direct post-Newtonian modulation of the phase of the signal which is induced by the tails of gravitational waves. The existence of tails is a well established prediction of general relativity. The tails are created by non-linear interaction between the time-varying multipole moments of the source (for instance, the quadrupole moment) and its static total mass  $M$  [12–19]. Physically, the waves undergo a continuous scattering, as they propagate outward from the source, off the Schwarzschild spacetime associated with  $M$ . This phenomenon is, in fact, common to the propagation of any integer spin field, like the electromagnetic field, on the Schwarzschild background [20–28]. In the gravitational case, the existence of tails is but one aspect of a fundamental property of the gravitational interaction, namely that its propagation proceeds both on and *within* the local light cone, i.e. at any velocity smaller than or equal (on average) to the velocity of light [29–35].

At large distances from the source (where the detector is located), the contribution of the wave tail is dominantly of post-Newtonian order  $\varepsilon^3$  with respect to the usual quadrupole radiation, where  $\varepsilon$  is the ratio of a typical velocity in the source and of the velocity of light. The wave tail, at this order, has been computed in [18, 36] and has been shown to be consistent, in the sense of energy conservation, with a related contribution [37, 38] in the radiation reaction forces acting within the source. The wave tail involves, besides the total mass  $M$ , the components of the quadrupole moment of the source integrated over the whole interval of time extending from arbitrary remote times in the past up to the retarded time  $t - r/c$  (this reflects the fact that gravity propagates, on average, at any velocity smaller than or equal to  $c$ ). Thus, the wave tail appears to be a *non-local* in time, or ‘hereditary’, functional of the source’s parameters. By contrast, the lowest-order post-Newtonian radiation (including the usual quadrupole radiation) is purely local, depending on the source’s parameters at time  $t - r/c$  only. We shall sometimes refer to the latter local component of the wave as the *wavefront*.

The Fourier transform of the wave tail at large distances from the source has a particularly simple form derived in [11] (see also [39, 40]). This form shows that both the *amplitude* and the *phase* of the wavefront are modified, in the Fourier domain, by small tail-induced corrections depending on the considered frequency. The modification of the amplitude of the wavefront has the consequence of modifying (by the famous ‘ $4\pi$ ’ term) the total averaged energy carried away from the source. In the case of an inspiralling binary, this implies an important ‘radiation reaction’ secular change of the phase of the signal (see, for example, [10]). This secular change of the phase is of formal order  $\varepsilon^3$ , which is the dominant post-Newtonian order of tails, times the total number of cycles left until the final coalescence, which is a large number of formal order  $\varepsilon^{-5}$ . By contrast, the ‘direct’ modification of the phase of the wavefront, as derived in [11, 39, 40], does not modify, in first approximation, the total averaged energy in the waves. It is therefore merely of post-Newtonian order  $\varepsilon^3$  in the phase of the waveform, being smaller than the ‘radiation reaction’ tail contribution by a factor  $\varepsilon^5$ . However, in spite of its smallness, this phase contribution represents an interesting effect. Notably, it has a characteristic dependence on frequency  $\sim \omega \ln \omega$ . In this paper we consider the practical detection of this effect in future

laser interferometric detectors, by the method of parameter estimation. As we shall see, the detection of this effect is challenging but not totally out of reach (at least for black-hole binaries). The possibility of detecting such a small effect shows the high potentiality of inspiralling compact binaries for performing tests of the non-linearity of general relativity.

By the method of parameter estimation we simply mean the estimation of the value of some parameter in the signal, independently of the values of the other parameters, by means of optimal signal processing. In our case, the convenient parameter is the total mass-energy  $M$  of the source which multiplies the tail contribution. This parameter is not independent, in the real signal, of the parameters of the wavefront since it is equal, for instance, to  $M = \mathcal{M}^{5/2}\mu^{-3/2}$ , where  $\mathcal{M}$  and  $\mu$  are the usual ‘chirp’ mass and reduced mass parametrizing the wavefront. However, in the filters, we can consider the total mass  $M$  multiplying the tail contribution as a test parameter which is *independent* of the other parameters. Maximizing the correlation by independently varying all these parameters, including  $M$ , yields a *test* of the existence of the tail contribution. Indeed, if this contribution does *not* exist, the optimal filter will be able to find a value of  $M$  which is compatible with zero, together with some definite values of the other parameters (e.g. the parameters  $\mathcal{M}$  and  $\mu$ ). On the contrary, if the contribution does exist, the optimal filter will measure a non-zero value of  $M$ , and it will be checked that this value is eventually consistent with the measured values of the parameters of the wavefront (see [42] for discussion).

With  $M$  considered as an independent parameter in the matched filters, we can compute, in the limit of high SNR, the anticipated one-sigma precision of its measurement (and thus of the measurement of the tail contribution itself) using the theory of the covariance matrix. Let us denote by  $\sigma_M^2 = C_{00}$  the variance of  $M$ , chosen to be the 00 component of the covariance matrix  $C_{\alpha\beta}$ , where the labels  $\alpha, \beta$  range over all the parameters. Then the tail contribution will be detected at the  $1 - \sigma$  confidence level when  $\sigma_M$  gets smaller than the value of  $M$  itself. In this paper we find that this happens when the optimal SNR of the signal is larger than a minimal value ranging from  $\sim 100$  to  $\sim 1000$  in the case of a model of white noise (depending on the number of independent parameters which are used in the filtering process), and ranging from  $\sim 280$  to  $\sim 2800$  in the case of a model of ‘coloured’ noise appropriate for shot noise in the standard recycling configuration of a laser interferometric detector with Fabry–Perot cavities. (The sensitive bandwidth of the detector is assumed to be 100–2000 Hz.) These figures are for a neutron-star binary with  $M = 2.8M_\odot$ . For a black-hole binary with  $M = 20M_\odot$ , the situation is much improved with minimal values of the SNR ranging from  $\sim 15$  to  $\sim 140$  (white noise), and from  $\sim 40$  to  $\sim 400$  (coloured noise).

We also perform a numerical simulation of the detection of the tail contribution, assuming that a preliminary (non-optimal) analysis has been performed on-line, yielding some preliminary values of the parameters of the wavefront. For simplicity, in this simulation we only use the minimal number of parameters. We construct a lattice of filters by the method of [43, 44] (one dimension in the lattice corresponds to the total mass  $M$ ), and we filter through it the output of the ‘detector’, composed of a known signal added to simulated Gaussian noise. By repeating the filtering process for a large number of realizations of noise, we obtain the distribution of the measured values of  $M$ , and, in particular, the standard deviation of the measured  $M$  around its mean. When the optimal SNR increases, the mean value tends to  $M$ , and the standard deviation tends to zero. Using the same criterion as above, we obtain minimal SNRs for detection of the tail contribution at the  $1 - \sigma$  level which are in good agreement with the analytical computations.

We think that the detection of the ‘direct’ tail-induced modulation of the phase of the wavefront is challenging but could be within reach in future laser interferometric detectors,

at least in the case of black-hole binaries. The number of coalescences of black holes is not known, but could be comparable with the number of coalescences of neutron stars [4]. Let us assume for discussion that three black-hole coalescences occur per year out to a distance of 200 Mpc, and furthermore that the currently planned VIRGO and LIGO detectors will observe these events with a SNR  $\sim 10$  (a reasonable value for black holes). Then, we can roughly estimate that VIRGO and LIGO will observe  $3\left(\frac{10}{40}\right)^3 = \frac{1}{20}$  events per year with a SNR larger than  $\sim 40$ , which is the least SNR required to detect the tail contribution in the case of black-hole binaries. This rate of events is too small, but it drastically depends on the statistics of events and on the shape of the detector noise spectrum. With the same assumptions concerning the statistics of events, we find that the advanced LIGO detector should detect tens of black-hole coalescences each year with a SNR larger than 40 (see, for example, equation (5.5) in Finn and Chernoff [9]).

The plan of this paper is as follows. In the next two sections we summarize some formulae concerning the generation of gravitational wave tails (section 2), and the theory of optimal signal processing (section 3). Section 4 is devoted to the analytical computation of the variance of the total mass  $M$  entering the tail contribution, and section 5 to our numerical simulation of its detection. The paper ends with an appendix.

## 2. Generation of gravitational wave tails

### 2.1. Case of a general isolated system

This subsection is a review of the relevant formulae (taken from [11, 36]) concerning the generation of gravitational wave tails by an isolated system, at large distances from the system where the detector is located. We shall denote by  $h(t)$  that particular combination of the components of the wave which is directly felt by the detector (e.g.  $h(t) = \delta L(t)/L$  is the relative variation of the arms' length of a laser interferometric detector), and we shall refer to it as the gravitational wave, or signal.

The wave  $h(t)$  is given, at the post-Newtonian order  $\varepsilon^3 \sim c^{-3}$  beyond the 'Newtonian' quadrupole radiation (where  $\varepsilon$  is the ratio of a typical velocity in the source and of the velocity of light), and at first order in the inverse of the distance  $r$  from the source, by the expression [36]

$$h(t) = h_0(t) + \frac{2GM}{c^3} \int_{-\infty}^t dt' \left[ \ln\left(\frac{t-t'}{2b}\right) + \frac{11}{12} \right] \frac{d^2 h_0}{dt'^2}(t'). \quad (2.1)$$

This expression is derived in a 'radiative' coordinate system, covering the regions at large distances from the source, and defined in (2.4) below. Throughout this paper, we shall work consistently with the precision at which (2.1) is valid. That is, we shall consistently neglect all terms of post-Newtonian order  $O(\varepsilon^4) = O(c^{-4})$  beyond the quadrupole radiation, and/or of order  $O(r^{-2})$  in the inverse of the distance from the source. Thus, for simplicity's sake, we shall not mention in (2.1), and in other formulae below, the neglected terms  $O(\varepsilon^4)$  and/or  $O(r^{-2})$ .

The wave  $h(t)$  is composed of two distinctive parts. The first part  $h_0(t)$  can be referred to as the 'wavefront'. It is defined by the equation

$$h_0(t) = \frac{G}{rc^4} \{F_+(p_i p_j - q_i q_j) + F_\times(p_i q_j + q_i p_j)\} \frac{d^2 K_{ij}}{dt^2}(t - r/c, \mathbf{n}) \quad (2.2)$$

where we denote by  $\mathbf{n}, \mathbf{p}, \mathbf{q}$  an oriented orthonormal triad, with  $\mathbf{n}$  the unit vector directed from the source towards the detector and  $\mathbf{p}, \mathbf{q}$  two unit polarization directions in the plane orthogonal to  $\mathbf{n}$ . The two coefficients  $F_+$  and  $F_\times$  denote the standard detector beam-pattern functions which are, for instance, given, in the case of a laser interferometric detector, by (104) of [1]. The tensor  $K_{ij}(u, \mathbf{n})$ , where  $u = t - r/c$  is the retarded time, is related to the (trace-free) multipole moments of the source (mass-type moments  $I_{ij}(u), I_{ijk}(u), \dots$  and current-type moments  $J_{ij}(u), J_{ijk}(u), \dots$ ) by

$$\begin{aligned} K_{ij}(u, \mathbf{n}) = & I_{ij}(u) + \frac{1}{c} \left[ \frac{1}{3} n_k I_{ijk}^{(1)}(u) + \frac{4}{3} \varepsilon_{kl(i} J_{j)k}(u) n_l \right] \\ & + \frac{1}{c^2} \left[ \frac{1}{12} n_k n_l I_{ijkl}^{(2)}(u) + \frac{1}{2} \varepsilon_{kl(i} J_{j)km}^{(1)}(u) n_l n_m \right] \\ & + \frac{1}{c^3} \left[ \frac{1}{60} n_k n_l n_m I_{ijklm}^{(3)}(u) + \frac{2}{15} \varepsilon_{kl(i} J_{j)kmn}^{(2)}(u) n_l n_m n_n \right]. \end{aligned} \quad (2.3)$$

(We denote  $I^{(n)}(u) = d^n I(u)/du^n$  and  $T_{(ij)} = \frac{1}{2}(T_{ij} + T_{ji})$ .) The multipole moments of the source are given at retarded time  $u$  by explicit integrals extending over the compact-supported stress-energy distribution of matter in the source at the *same* retarded time  $u$ . The expressions of the moments of the source are given in [46, 47] (see also [11, 36]). In the limit  $c \rightarrow \infty$ , the tensor (2.3) reduces to the usual Newtonian quadrupole moment of the source.

The second part in the wave  $h(t)$ , which is purely of post-Newtonian order  $\varepsilon^3$ , can be referred to as the 'wave tail'. As is clear from its expression, the wave tail is, in contrast with the wavefront, a *non-local* in time functional of the stress-energy tensor of the source, depending on its values not only at the simply retarded time  $u = t - r/c$ , but also at all times anterior or equal to  $u$ . (Note that the precision given by the first term in (2.3) is sufficient to compute the wave tail, which is already of small order  $\varepsilon^3$ .) Subject to weak conditions concerning the emission of radiation at very early times  $t' \rightarrow -\infty$ , one can easily show that the wave tail in (2.1) is given as a convergent integral (see [11, 36, 37]). We have chosen, following [11], to include the term corresponding to the constant  $\frac{11}{12}$  in the wave tail although this term is, in fact, a local functional of the source. The constant  $b$ , in the logarithm of the integrand of the wave tail, is an arbitrary positive constant having the dimension of time. It enters the relation between the radiative coordinate system  $t, r$  used by the experimenters at large distances from the source and the harmonic coordinate system  $t_H, r_H$  covering the source:

$$t = t_H - \frac{2GM}{c^3} \ln \left( \frac{r_H}{cb} \right) \quad (2.4a)$$

$$r = r_H. \quad (2.4b)$$

By substituting (2.4) into (2.1), we eliminate the dependence on the constant  $b$  [36]. (Note that the value of the constant  $\frac{11}{12}$  depends on the coordinate system chosen in (2.4) to cover the source. For instance, the value is  $\frac{17}{12}$  instead of  $\frac{11}{12}$  if we use in (2.4) Schwarzschild coordinates  $t_S, r_S$  instead of harmonic coordinates  $t_H, r_H$ ; compare [11] and the work of Poisson [39].)

The Fourier transform of the gravitational wave  $h(t)$  has been derived in [11]. Let us denote by  $\tilde{h}(\omega)$  and  $\tilde{h}_0(\omega)$  the Fourier transforms of  $h(t)$  and of its wavefront  $h_0(t)$  (where  $\omega = 2\pi f$  denotes the angular frequency):

$$\tilde{h}(\omega) = \int_{-\infty}^{+\infty} dt h(t) e^{i\omega t} \quad \tilde{h}_0(\omega) = \int_{-\infty}^{+\infty} dt h_0(t) e^{i\omega t}. \quad (2.5)$$

Since  $h(t)$  and  $h_0(t)$  are real, we have  $\tilde{h}(-\omega) = \tilde{h}^*(\omega)$  and  $\tilde{h}_0(-\omega) = \tilde{h}_0^*(\omega)$  where  $*$  denotes the complex conjugation. Then, by taking the Fourier transform of (2.1), one obtains

$$\tilde{h}(\omega) = \tilde{h}_0(\omega) \left\{ 1 + \frac{2GM}{c^3} \left[ \frac{1}{2}\pi|\omega| + i\omega \ln(2|\omega|b') \right] \right\} \quad (2.6)$$

where  $|\omega|$  denotes the absolute value of  $\omega$ , and where the constant  $b'$  is related to the constant  $b$  by

$$b' = b \exp \left[ C - \frac{11}{12} \right] \quad (2.7)$$

with  $C$  denoting the Euler constant  $C = 0.577 \dots$ . (Note that the expression (2.6) is only valid for low frequencies  $\omega$  such that  $GM\omega/c^3$  is of small post-Newtonian order  $O(\epsilon^3)$ .)

The tail-induced corrections in (2.6) imply a modification of both the amplitude and the phase of the wavefront in the Fourier domain. In particular, the modification of the *phase* of the wavefront, as given by the imaginary part of the brackets in (2.6), introduces a new effect in the case where the radiation contains more than one frequency in the Fourier domain (see [11]). This effect can be rigorously analysed when the radiation spectrum is composed of several well separated wavepackets. Two wavepackets, centred around two different frequencies  $\omega_1$  and  $\omega_2$  (and belonging to the 'same' wave), propagate with the same group velocity, but their relative positions are slightly shifted along the line of sight. (The position of the wavepacket is the position of its maximum of amplitude in space.) They differ by a small quantity equal to  $2GM/c^2$  times the difference of the *logarithms* of their central frequencies  $\omega_1$  and  $\omega_2$ . Put another way, the two wavepackets arrive at a given distance from the source with a small relative delay equal to  $(2GM/c^3) \ln(\omega_1/\omega_2)$ , with the wavepacket corresponding to the lower frequency arriving first. In a sense, only this effect should be regarded as the tail effect.

In this paper, we shall make a definite choice of the constant  $b'$  appearing in (2.6) (and thus a choice of a particular radiative coordinate system). We shall relate  $b'$  to the 'seismic cut-off' of a laser interferometric detector, defined to be the frequency  $\omega_s$  below which the terrestrial seismic noise prevents any detection, by posing

$$b' = \frac{1}{2\omega_s}. \quad (2.8)$$

(In a more general situation, we can simply think of  $\omega_s$  as being a typical frequency at which the detector is operating.)

## 2.2. Application to inspiralling compact binaries

Recall that the wave generation formalism of [36], on which the expression of the wave tail in (2.1) is based, is valid for systems of compact objects like inspiralling compact binaries, which can be modelled by two point masses moving on an inspiralling circular orbit. We shall consider for this application only the dominant frequency component of the radiation, equal to two times the orbital frequency of the binary. In this case, the wavefront  $h_0(t)$  is of the form

$$h_0(t) = A(\Omega(t)) \cos[\varphi(t)] \quad (2.9)$$

where  $\Omega(t)$  is twice the orbital frequency,  $\varphi(t)$  denotes the instantaneous phase of the signal, satisfying  $d\varphi(t)/dt \equiv \dot{\varphi}(t) = \Omega(t)$ , and  $A(\Omega(t))$  is some instantaneous amplitude.

The Fourier transform of the wavefront (2.9) can be computed by means of the stationary phase approximation method, valid in the 'adiabatic' regime of the inspiral of the orbit during which the relative changes of the instantaneous frequency  $\Omega(t)$  of the radiation in *one* corresponding period are small, for example,  $\dot{\Omega}(t) \ll \Omega^2$ . As a result, we have (see [9])

$$\tilde{h}_0(\omega) = \frac{1}{2} \sqrt{\frac{2\pi}{\dot{\Omega}(T)}} A(\omega) \exp \left\{ i \left[ \omega T - \varphi(T) - \frac{1}{4}\pi \right] \right\} \quad (2.10)$$

where  $T$  denotes the particular instant at which  $\Omega(T) = \omega$ . The expression (2.10) is written for  $\omega > 0$ ; for  $\omega < 0$ , we use  $\tilde{h}_0(\omega) = \tilde{h}_0^*(-\omega)$ . Now the rate of inspiral of the orbit is governed by radiation reaction effects (in reaction to the emission of gravitational waves), or equivalently by the energy balance equation  $dE/dt = -\mathcal{L}$  relating the orbital binding energy  $E$  of the binary (at some frequency  $\Omega$ ) to the total averaged power, or luminosity  $\mathcal{L}$  of the gravitational wave emission (at the same frequency  $\Omega$ ). From this equation we deduce the quantities needed to compute (2.10), namely

$$\frac{1}{\dot{\Omega}(T)} = -\frac{1}{\mathcal{L}(\omega)} \frac{dE}{d\Omega}(\omega) \quad (2.11)$$

and

$$\omega T - \varphi(T) = \omega t_c - \varphi_c + \int_{\omega}^{+\infty} \frac{\omega - \Omega}{\mathcal{L}(\Omega)} \frac{dE}{d\Omega}(\Omega) d\Omega. \quad (2.12)$$

We denote by  $t_c$  the instant of coalescence (at which the frequency goes formally to infinity), and by  $\varphi_c$  the corresponding final phase.

The binding energy  $E$  is known from the equations of motion of two point masses moving on a circular orbit, while the luminosity  $\mathcal{L}$  is computed by differentiating, squaring and averaging the gravitational field at large distances from the source. We shall use the expressions for  $E$  and  $\mathcal{L}$  which are valid with the inclusion of all post-Newtonian terms up to  $\varepsilon^3$ . These expressions are

$$E(\Omega) = -\frac{1}{2} \mu c^2 \left( \frac{GM\Omega}{2c^3} \right)^{2/3} \left\{ 1 + \left( -\frac{3}{4} - \frac{1}{12}\nu \right) \left( \frac{GM\Omega}{2c^3} \right)^{2/3} \right\} \quad (2.13)$$

where  $\mu$  is the reduced mass of the binary and  $\nu = \mu/M$ , and

$$\mathcal{L}(\Omega) = \frac{32c^5}{5G} \left( \frac{GM\Omega}{2c^3} \right)^{10/3} \left\{ 1 + \left( -\frac{1247}{336} - \frac{35}{12}\nu \right) \left( \frac{GM\Omega}{2c^3} \right)^{2/3} + 2\pi \frac{GM\Omega}{c^3} \right\} \quad (2.14)$$

where  $\mathcal{M} = \mu^{3/5} M^{2/5}$  is the chirp mass of the binary. The post-Newtonian correction  $\varepsilon^3$  in  $\mathcal{L}$  is directly due to the real part of the brackets in (2.6), i.e. to the *amplitude* modulation of the wavefront induced by the tail itself [39]. We shall refer to this correction  $\varepsilon^3$  as the 'radiation reaction' tail contribution.

By inserting (2.13) and (2.14) into (2.11) and (2.12) we obtain an explicit expression for the Fourier transform (2.10) of the wavefront. *A priori*, this expression contains a 'radiation reaction' tail contribution in both its amplitude and its phase. However, inspection of (2.11) and (2.14) readily shows that the 'radiation reaction' tail contribution in the amplitude of the

wavefront is, in fact, exactly cancelled by the real part of the brackets in (2.6). Accordingly, we find it convenient to write the wave (2.6) in the form

$$\tilde{h}(\omega) = \tilde{H}_0(\omega) \left\{ 1 + i \frac{2GM\omega}{c^3} \ln(|\omega|/\omega_s) \right\} \quad (2.15)$$

where we retain in the brackets only the 'direct' tail-induced modulation of the phase (with our choice (2.8) for the constant  $b'$ ). Assuming, as usual, that the post-Newtonian corrections in the amplitude of  $\tilde{H}_0(\omega)$  are negligible, we can now use

$$A(\omega) = \mathcal{A} \frac{GM}{c^3} \left( \frac{4GM\omega}{c^3} \right)^{2/3} \quad (2.16)$$

where the amplitude parameter  $\mathcal{A}$  is given by

$$\mathcal{A} = \frac{c}{2r} \left\{ F_+^2 (1 + \cos^2 \iota)^2 + 4F_x^2 \cos^2 \iota \right\}^{1/2} \quad |\mathcal{A}| \leq \frac{c}{r} \quad (2.17)$$

where  $F_+$  and  $F_x$  are the detector beam-pattern functions appearing in (2.2), and  $\iota$  is the angle between the line of sight from the source to the detector and the normal to the orbital plane. Finally we obtain

$$\tilde{H}_0(\omega) = \frac{1}{8} \sqrt{5\pi} \mathcal{A} \eta^{-1/2} \omega^{-7/6} \exp \left\{ i \left[ \omega t_c - \varphi_c - \frac{1}{4}\pi + \eta \omega^{-5/3} + \lambda \omega^{-1} + \gamma \omega^{-2/3} \right] \right\} \quad (2.18)$$

where for later convenience we have introduced the parameters

$$\eta = \frac{3}{4} \left( \frac{c^3}{4GM} \right)^{5/3} \quad (2.19a)$$

$$\lambda = \frac{5}{48} \left( \frac{743}{336} + \frac{11}{4} \nu \right) \left( \frac{c^3}{G\mu} \right) \quad (2.19b)$$

$$\gamma = -\frac{3\pi}{2\nu} \left( \frac{c^3}{4GM} \right)^{2/3} \quad (2.19c)$$

The 'radiation reaction' tail contribution in (2.18) is the term  $\gamma \omega^{-2/3}$ . Note that for *spinless* objects, the parameter  $\gamma$  is not independent of  $\eta$  and  $\lambda$ . However, when the two (compact) stars are rotating,  $\gamma$  receives an additional contribution  $\beta$  depending on the two spins of the stars and on the total angular momentum of the binary [51]. This contribution  $\beta$  can be assumed to be constant, and modifies  $\gamma$  as follows:

$$\gamma = \frac{3}{8\nu} (\beta - 4\pi) \left( \frac{c^3}{4GM} \right)^{2/3} \quad (2.19c')$$

In this case,  $\gamma$  is independent of the other parameters  $\eta$  and  $\lambda$ .

Finally, let us consider the 'direct' tail-induced modulation of the phase of the waveform in the brackets of (2.15), i.e.

$$\theta(\omega) = \frac{2GM\omega}{c^3} \ln(|\omega|/\omega_s). \quad (2.20)$$

As is clear from (2.15), (2.18) and (2.19a), this phase modulation is smaller by a factor of order  $\eta^{-1} \sim \varepsilon^5$  than the 'radiation reaction' contribution of the tail in (2.18). However,  $\theta(\omega)$  has a very distinctive dependence on frequency ( $\sim \omega \ln \omega$ ) which could make it more easily identifiable in the real signal than the 'radiation reaction' tail contribution. On the other hand, the 'radiation reaction' contribution is plagued in the real signal with the spin-orbit contribution  $\beta$  (see (2.19c')), and it is not clear how it could be detected without ambiguity. Thus we shall focus our attention on the 'direct' tail-induced contribution  $\theta(\omega)$ , and shall investigate the level at which it could be detected in future gravitational wave interferometers.

### 3. Summary of optimal filtering techniques

This section is intended to provide well known formulae about the theory of optimal filtering (see the book of Wainstein and Zubakov [45] and, in the context of gravitational radiation, [1, 43, 44, 48–50]), which we shall use in sections 4 and 5. The raw output of the detector  $o(t)$  is the superposition of the useful signal  $h(t)$  given by (2.1) and of noise  $n(t)$ :

$$o(t) = h(t) + n(t). \quad (3.1)$$

The noise is assumed to be a stationary Gaussian random variable, with zero expectation value

$$\overline{n(t)} = 0 \quad (3.2)$$

and with (supposedly known) frequency-dependent power spectral density  $S_h(\omega)$  satisfying

$$\overline{\tilde{n}(\omega)\tilde{n}^*(\omega')} = 2\pi\delta(\omega - \omega')S_h(\omega) \quad (3.3)$$

where  $\tilde{n}(\omega)$  is the Fourier transform of  $n(t)$  in convention (2.5). In (3.2) and (3.3), we denote by an upper bar the average over many realizations of noise in a large ensemble of detectors. From (3.3), we have  $S_h(\omega) = S_h^*(\omega) = S_h(-\omega) > 0$ .

Looking for the useful signal  $h(t)$  in the output of the detector  $o(t)$ , the experimenters construct the correlation  $c(t)$  between  $o(t)$  and a filter  $q(t)$ , i.e.

$$c(t) = \int_{-\infty}^{+\infty} dt' o(t')q(t+t') \quad (3.4)$$

and divide  $c(t)$  by the square root of its variance (or correlation noise). Thus, the experimenters consider the ratio

$$\sigma[q](t) = \frac{c(t)}{(\overline{c^2(t)} - \overline{c(t)}^2)^{1/2}} = \frac{\int_{-\infty}^{+\infty} (1/2\pi) d\omega \tilde{o}(\omega)\tilde{q}^*(\omega)e^{i\omega t}}{(\int_{-\infty}^{+\infty} (1/2\pi) d\omega S_h(\omega)|\tilde{q}(\omega)|^2)^{1/2}} \quad (3.5)$$

where  $\tilde{o}(\omega)$  and  $\tilde{q}(\omega)$  are the Fourier transforms of  $o(t)$  and  $q(t)$ . The expectation value (or ensemble average) of this ratio defines the filtered signal-to-noise ratio (SNR)

$$\rho[q](t) = \overline{\sigma[q](t)} = \frac{\int_{-\infty}^{+\infty} (1/2\pi) d\omega \tilde{h}(\omega)\tilde{q}^*(\omega)e^{i\omega t}}{(\int_{-\infty}^{+\infty} (1/2\pi) d\omega S_h(\omega)|\tilde{q}(\omega)|^2)^{1/2}}. \quad (3.6)$$

The optimal filter (or Wiener filter) which maximizes the SNR (3.6) at a particular instant  $t = 0$  (say), is given by the matched filtering theorem as

$$\tilde{q}(\omega) = \gamma \frac{\tilde{h}(\omega)}{S_h(\omega)} \quad (3.7)$$

where  $\gamma$  is an arbitrary real constant. The optimal filter (3.7) is matched on the expected signal  $\tilde{h}(\omega)$  itself, and weighted by the inverse of the power spectral density of the noise. The maximum SNR, corresponding to the optimal filter (3.7), is given by

$$\rho = \left( \int_{-\infty}^{+\infty} \frac{d\omega}{2\pi} \frac{|\tilde{h}(\omega)|^2}{S_h(\omega)} \right)^{1/2} = \langle h, h \rangle^{1/2}. \quad (3.8)$$

This is the best achievable SNR with a linear filter. In (3.8), we have used, for any two real functions  $f(t)$  and  $g(t)$ , the notation

$$\langle f, g \rangle = \int_{-\infty}^{+\infty} \frac{d\omega}{2\pi} \frac{\tilde{f}(\omega)\tilde{g}^*(\omega)}{S_h(\omega)} \quad (3.9)$$

for an inner scalar product satisfying  $\langle f, g \rangle = \langle f, g \rangle^* = \langle g, f \rangle$ .

In practice, the signal  $h(t)$  or  $\tilde{h}(\omega)$  is of known form (given by (2.1) or (2.6)) but depends on an unknown set of parameters which describe the source of radiation, and are to be measured. The experimenters must therefore use a whole family of filters analogous to (3.7) but in which the signal is parametrized by a whole family of 'test' parameters which are *a priori* different from the actual source parameters. Thus, one will have to define and use a *lattice* of filters in the parameter space (see section 5). The set of parameters maximizing the SNR (3.6) is equal, by the matched filtering theorem, to the set of source parameters. However, in a single detector, the experimenters maximize the ratio (3.5) rather than the SNR (3.6), and therefore make errors on the determination of the parameters, depending on a particular realization of noise in the detector. If the SNR is high enough, the measured values of the parameters are Gaussianly distributed around the source parameters, with variances and correlation coefficients given by the standard covariance matrix, the computation of which we now recall. Since the optimal filter (3.7) is defined up to an arbitrary multiplicative constant, it is convenient to treat separately a constant amplitude parameter in front of the signal (involving, for instance, the distance of the source). We shall thus write the signal in the form

$$\tilde{h}(\omega; \mathcal{A}, \lambda_\alpha) = \mathcal{A} \tilde{k}(\omega; \lambda_\alpha) \quad (3.10)$$

where  $\mathcal{A}$  is an amplitude parameter given, for instance, by (2.17). The function  $\tilde{k}$  depends only on the other parameters, collectively denoted by  $\lambda_\alpha$  where the Greek label  $\alpha$  ranges for later convenience on the values  $0, 1, \dots, N$ . The family of matched filters (or 'templates') we consider is defined by

$$\tilde{q}(\omega; {}_t\lambda_\alpha) = \gamma' \frac{\tilde{k}(\omega; {}_t\lambda_\alpha)}{S_h(\omega)} \quad (3.11)$$

where  ${}_t\lambda_\alpha$  is a set of test parameters and  $\gamma'$  is arbitrary. (In section 5 we shall make a suitable choice of  $\gamma'$  so as to simplify the numerical simulation.) Note that these parameters are assumed to be all independent, even though the source parameters  $\lambda_\alpha$  may not be so. By substituting (3.11) into (3.5) and choosing  $t = 0$ , we get, with the notation (3.9),

$$\sigma({}_t\lambda) = \frac{\langle o, k({}_t\lambda) \rangle}{\langle k({}_t\lambda), k({}_t\lambda) \rangle^{1/2}} \quad (3.12)$$

(Note that  $\sigma$  is, in fact, a function of both the parameters  $\lambda_\alpha$  and  ${}_t\lambda_\alpha$ .) Now the experimenters choose as their best estimate of the source parameters  $\lambda_\alpha$  the *measured* parameters  ${}_m\lambda_\alpha$  which among all the test parameters  ${}_t\lambda_\alpha$  (independently) maximize (3.12), i.e. which satisfy

$$\frac{\partial \sigma}{\partial {}_t\lambda_\alpha}({}_m\lambda) = 0 \quad \alpha = 0, 1, \dots, N. \quad (3.13)$$

Assuming that the SNR is high enough, we can work out (3.13) up to the first order in the difference between the actual source parameters and the measured ones,

$$\delta\lambda_\alpha = \lambda_\alpha - {}_m\lambda_\alpha. \quad (3.14)$$

As a result, we obtain

$$\delta\lambda_\alpha = C_{\alpha\beta} \left\{ - \left\langle n, \frac{\partial h}{\partial \lambda_\beta} \right\rangle + \frac{\langle n, h \rangle}{\langle h, h \rangle} \left\langle h, \frac{\partial h}{\partial \lambda_\beta} \right\rangle \right\} \quad (3.15)$$

where a summation is understood on the dummy label  $\beta$ , and where the matrix  $C_{\alpha\beta}$  (with  $\alpha, \beta = 0, 1, \dots, N$ ) is the inverse of the Fisher information matrix

$$D_{\alpha\beta} = \left\langle \frac{\partial h}{\partial \lambda_\alpha}, \frac{\partial h}{\partial \lambda_\beta} \right\rangle - \frac{1}{\langle h, h \rangle} \left\langle h, \frac{\partial h}{\partial \lambda_\alpha} \right\rangle \left\langle h, \frac{\partial h}{\partial \lambda_\beta} \right\rangle \quad (3.16)$$

(we have  $C_{\alpha\beta} D_{\beta\gamma} = \delta_{\alpha\gamma}$ ). In the right-hand sides of (3.15) and (3.16), the signal is equally (with this approximation) parametrized by the measured or actual parameters. Since the noise is Gaussian, so are, by (3.15), the variables  $\delta\lambda_\alpha$ s (indeed, the  $\delta\lambda_\alpha$ s result from a linear operation on the noise variable). The expectation value and quadratic moments of the distribution of these variables are readily obtained from the facts that  $\langle n, f \rangle = 0$  and  $\langle n, f \rangle \langle n, g \rangle = \langle f, g \rangle$  for any deterministic functions  $f$  and  $g$  (see (3.2) and (3.3)). We then obtain

$$\overline{\delta\lambda_\alpha} = 0 \quad (3.17)$$

$$\overline{\delta\lambda_\alpha \delta\lambda_\beta} = C_{\alpha\beta}. \quad (3.18)$$

Thus, the matrix  $C_{\alpha\beta}$  (inverse of (3.16)) is the matrix of variances and correlation coefficients, or covariance matrix, of the variables  $\delta\lambda_\alpha$ . The probability distribution of the  $\delta\lambda_\alpha$ s reads as

$$P(\delta\lambda_\alpha) = \frac{1}{\sqrt{(2\pi)^{N+1} \det C}} \exp \left\{ -\frac{1}{2} D_{\alpha\beta} \delta\lambda_\alpha \delta\lambda_\beta \right\} \quad (3.19)$$

where  $\det C$  is the determinant of  $C_{\alpha\beta}$ . A similar analysis can be done for the measurement of the amplitude parameter  $\mathcal{A}$  of the signal.

#### 4. Analytical investigation of the detection of the tail contribution

The gravitational wave signal  $\tilde{h}(\omega)$  is now explicitly supposed to be of the form (2.15), i.e. constituted by  $\tilde{H}_0(\omega)$  (that we shall slightly abusively refer to as the wavefront) and corrected by the tail-induced phase modulation  $\theta(\omega)$ , the latter having in factor the total mass  $M$  of the source. It is convenient to assume that  $M$  itself is one of the parameters  $\lambda_\alpha$  of the signal. We shall keep the value 0 of the Greek label  $\alpha$  for the total mass  $M$ , so that  $\lambda_0 = M$ , and shall introduce Latin labels  $i, j = 1, \dots, N$  for the parameters in  $\tilde{H}_0(\omega)$ . Thus we denote  $\lambda_\alpha = \{M, \lambda_i\}$  and write (2.15) as

$$\tilde{h}(\omega; \mathcal{A}, \lambda_\alpha) = \tilde{H}_0(\omega; \mathcal{A}, \lambda_i) \left\{ 1 + i \frac{2GM\omega}{c^3} \ln(|\omega|/\omega_s) \right\} \quad (4.1)$$

where

$$\tilde{H}_0(\omega; \mathcal{A}, \lambda_i) = \mathcal{A} \tilde{K}_0(\omega; \lambda_i). \quad (4.2)$$

Evidently, the total mass  $M$  may not be independent, in the real signal, of the parameters  $\lambda_i$ . However, in the method of parameter estimation, it is important to take the correlation of the output of the detector with a family of matched filters (3.11) depending on test parameters  ${}_\iota\lambda_\alpha = \{{}_\iota M, {}_\iota\lambda_i\}$  where  ${}_\iota M$  is independent of the other parameters  ${}_\iota\lambda_i$ . This way of proceeding permits a test of the existence of  $\theta(\omega)$  in the real signal.

4.1. *Computation of the variance of M*

The covariance matrix of the signal  $C_{\alpha\beta}$ , inverse of the matrix  $\mathcal{D}_{\alpha\beta}$  defined by (3.16), will give us the level at which it will be possible to detect the tail contribution in (4.1). The differentiation of (4.1) with respect to the parameters  $M$  and  $\lambda_i$  is easily performed, and yields

$$\frac{1}{\tilde{h}} \frac{\partial \tilde{h}}{\partial M} = i \frac{2G\omega}{c^3} \ln(|\omega|/\omega_s) + O(G^2) \tag{4.3a}$$

$$\frac{1}{\tilde{h}} \frac{\partial \tilde{h}}{\partial \lambda_i} = \frac{1}{\tilde{H}_0} \frac{\partial \tilde{H}_0}{\partial \lambda_i} . \tag{4.3b}$$

For the sake of clarity in the derivation of the covariance matrix, we indicate by  $O(G^n)$  some negligible terms of the order of  $n$  times the tail term (which carries the constant  $G$  in front). In terms of the post-Newtonian parameter  $\epsilon$  we have  $O(G^n) = O(\epsilon^{3n})$ . With the help of (4.3), we can work out the components of  $\mathcal{D}_{\alpha\beta}$  at leading order in  $G$  (i.e. at leading order in  $\epsilon^3$  following our notation). We find, separating the label  $\alpha = 0$  corresponding to the parameter  $M$  from the Latin labels  $i, j$  corresponding to the parameters of the wavefront (and showing explicitly the dependence in  $G/c^3$ ),

$$\mathcal{D}_{00} = \frac{G^2}{c^6} \mathcal{D}_{00}^{(2)} + O(G^3) \tag{4.4a}$$

$$\mathcal{D}_{0i} = \frac{G}{c^3} \mathcal{D}_{0i}^{(1)} + O(G^2) \tag{4.4b}$$

$$\mathcal{D}_{ij} = \mathcal{D}_{ij}^{(0)} + O(G) \tag{4.4c}$$

where the coefficients are given by the formulae

$$\mathcal{D}_{00}^{(2)} = 4 \int_0^{+\infty} \frac{d\omega \omega^2}{\pi S_h(\omega)} |\tilde{H}_0(\omega)|^2 \ln^2(\omega/\omega_s) \tag{4.5}$$

$$\mathcal{D}_{0i}^{(1)} = 2 \text{Im} \int_0^{+\infty} \frac{d\omega \omega}{\pi S_h(\omega)} \tilde{H}_0^*(\omega) \frac{\partial \tilde{H}_0}{\partial \lambda_i} \ln(\omega/\omega_s) \tag{4.6}$$

(Im denotes the imaginary part), and

$$\mathcal{D}_{ij}^{(0)} = \left\langle \frac{\partial H_0}{\partial \lambda_i}, \frac{\partial H_0}{\partial \lambda_j} \right\rangle - \frac{1}{\rho_0^2} \left\langle H_0, \frac{\partial H_0}{\partial \lambda_i} \right\rangle \left\langle H_0, \frac{\partial H_0}{\partial \lambda_j} \right\rangle . \tag{4.7}$$

As we see,  $\mathcal{D}_{ij}^{(0)}$  is the information matrix of wavefront  $\tilde{H}_0$  alone, whose inverse,  $\mathcal{C}_{ij}^{(0)}$  say, is the covariance matrix of  $\tilde{H}_0$ . In (4.7) we denote by  $\rho_0$  the optimal SNR associated with  $\tilde{H}_0$ , i.e.

$$\rho_0 = \langle H_0, H_0 \rangle^{1/2} . \tag{4.8}$$

The matrix (4.4), in which we have (4.5)–(4.8), must now be inverted. We perform the computation at leading order in  $G/c^3$  and express the result in terms of the coefficients  $\mathcal{D}_{00}^{(2)}$  and  $\mathcal{D}_{0i}^{(1)}$  given by (4.5) and (4.6), and in terms of the components of the covariance

matrix  $C_{ij}^{(0)}$  of the wavefront, satisfying  $C_{ij}^{(0)} D_{jk}^{(0)} = \delta_{ik}$  where  $D_{ij}^{(0)}$  is given by (4.7). A short computation gives

$$C_{00} = \frac{c^6}{G^2} \left\{ \frac{1}{D_{00}^{(2)} - D_{0k}^{(1)} D_{0l}^{(1)} C_{kl}^{(0)}} + O(G) \right\} \quad (4.9a)$$

$$C_{0i} = \frac{c^3}{G} \left\{ \frac{-D_{0j}^{(1)} C_{ij}^{(0)}}{D_{00}^{(2)} - D_{0k}^{(1)} D_{0l}^{(1)} C_{kl}^{(0)}} + O(G) \right\} \quad (4.9b)$$

$$C_{ij} = C_{ij}^{(0)} + \frac{D_{0m}^{(1)} D_{0n}^{(1)} C_{im}^{(0)} C_{jn}^{(0)}}{D_{00}^{(2)} - D_{0k}^{(1)} D_{0l}^{(1)} C_{kl}^{(0)}} + O(G). \quad (4.9c)$$

We can then express this result in terms of  $D_{00}$  and  $D_{0i}$  (and still  $C_{ij}^{(0)}$ ) rather than in terms of  $D_{00}^{(2)}$  and  $D_{0i}^{(1)}$ . This reintroduces further negligible terms in  $G/c^3$ . However, now that the derivation of the result is done, we simply skip all indications  $O(G^n)$  of negligible terms. Hence we obtain, with the required precision, the final expressions

$$C_{00} = \frac{1}{D_{00} - D_{0k} D_{0l} C_{kl}^{(0)}} \quad (4.10a)$$

$$C_{0i} = \frac{-D_{0j} C_{ij}^{(0)}}{D_{00} - D_{0k} D_{0l} C_{kl}^{(0)}} \quad (4.10b)$$

$$C_{ij} = C_{ij}^{(0)} + \frac{D_{0m} D_{0n} C_{im}^{(0)} C_{jn}^{(0)}}{D_{00} - D_{0k} D_{0l} C_{kl}^{(0)}}. \quad (4.10c)$$

These expressions, together with the explicit formulae for  $D_{00}$  and  $D_{0i}$  computed from (4.5) and (4.6), and the knowledge of the covariance matrix  $C_{ij}^{(0)}$  of the wavefront (inverse of (4.7)), give the variances and correlation coefficients of the variables  $\delta\lambda_\alpha = \lambda_\alpha - m\lambda_\alpha$ . In particular, by integrating the probability distribution (3.19) over the variables  $\delta\lambda_i = \lambda_i - m\lambda_i$  of the wavefront, we obtain the probability distribution of the variable

$$\delta M = M - m M \quad (4.11)$$

which is the difference between the actual and measured total masses parametrizing the wave tail:

$$P(\delta M) = \frac{1}{\sqrt{2\pi\sigma_M^2}} \exp \left\{ -\frac{\delta M^2}{2\sigma_M^2} \right\} \quad (4.12)$$

where the variance  $\sigma_M^2$  (square of the standard deviation  $\sigma_M$ ) is given by

$$\sigma_M^2 = C_{00} = \frac{1}{D_{00} - D_{0i} D_{0j} C_{ij}^{(0)}}. \quad (4.13)$$

#### 4.2. Application to inspiralling compact binaries

To compute  $\sigma_M$  for inspiralling compact binaries, we need to substitute into (4.13) the expression (2.18) of the wavefront  $\tilde{H}_0$ , which is (for  $\omega > 0$ )

$$\tilde{H}_0(\omega) = \frac{1}{8}\sqrt{5\pi}\mathcal{A}\eta^{-1/2}\omega^{-7/6} \exp\left\{i\left[\omega t_c - \varphi_c - \frac{1}{4}\pi + \eta\omega^{-5/3} + \lambda\omega^{-1} + \gamma\omega^{-2/3}\right]\right\}. \quad (4.14)$$

The parameters  $\eta$ ,  $\lambda$ , and  $\gamma$ , given by (2.19), are associated respectively with the dominant radiation reaction, with the post-Newtonian correction  $\varepsilon^2$  involving the mass ratio  $\nu = \mu/M$ , and with the post-Newtonian correction  $\varepsilon^3$  involving the spin-orbit term  $\beta$  and the ‘radiation reaction’ tail contribution. The SNR  $\rho_0$  associated with (4.14) is readily obtained by inserting (4.14) into (4.8). We find

$$\rho_0^2 = \langle h_0, h_0 \rangle = \frac{5}{64}\mathcal{A}^2\eta^{-1}f_{7/3} \quad (4.15)$$

where we use the definition, for any  $\alpha$ , of the moments

$$f_\alpha = \int_0^{+\infty} \frac{d\omega \omega^{-\alpha}}{S_h(\omega)}. \quad (4.16)$$

The covariance matrix  $C_{ij}^{(0)}$  of (4.14), inverse of (4.7), is now computed. *A priori*, the wavefront (4.14) contains five independent parameters relevant to the construction of filters, which are  $\lambda_i = \{\eta, \varphi_c, t_c, \lambda, \gamma\}$ . However, if we know *a priori* that the spins of the stars are negligible, then we can consider only the four parameters  $\lambda_i = \{\eta, \varphi_c, t_c, \lambda\}$ ; and if, furthermore, we know some relation between the two masses of the binary (for instance that they are nearly equal), then  $\lambda_i = \{\eta, \varphi_c, t_c\}$  is sufficient. Since the level at which the detection of  $\theta(\omega)$  becomes possible strongly depends on the number of independent parameters in the filtering process [53], we shall perform the computation for the three cases where we consider 3, 4 or 5 independent parameters in (4.14) (totalizing with  $M$  in front of the tail contribution 4, 5 or 6 parameters in the complete waveform). The logarithmic derivatives of (4.14) with respect to the  $\lambda_i$ s are given by

$$\frac{1}{\tilde{H}_0} \frac{\partial \tilde{H}_0}{\partial \eta} = -\frac{1}{2\eta} + i\omega^{-5/3} \quad (4.17a)$$

$$\frac{1}{\tilde{H}_0} \frac{\partial \tilde{H}_0}{\partial \varphi_c} = -i \quad (4.17b)$$

$$\frac{1}{\tilde{H}_0} \frac{\partial \tilde{H}_0}{\partial t_c} = i\omega \quad (4.17c)$$

$$\frac{1}{\tilde{H}_0} \frac{\partial \tilde{H}_0}{\partial \lambda} = i\omega^{-1} \quad (4.17d)$$

$$\frac{1}{\tilde{H}_0} \frac{\partial \tilde{H}_0}{\partial \gamma} = i\omega^{-2/3}. \quad (4.17e)$$

By substituting these expressions into (4.7), we obtain the covariance matrix in the form

$$C_{ij}^{(0)} = \frac{f_{7/3}}{\rho_0^2} F_{ij} \quad (4.18)$$

where  $\rho_0^2$  is given by (4.15), and where the matrix  $F_{ij}$  is the inverse matrix of the matrix  $E_{ij}$  defined in terms of the moments (4.16) by

$$E_{ij} = \begin{pmatrix} f_{17/3} & -f_4 & f_3 \\ -f_4 & f_{7/3} & -f_{4/3} \\ f_3 & -f_{4/3} & f_{1/3} \end{pmatrix} \quad (3 \text{ parameters}) \quad (4.19a)$$

$$E_{ij} = \begin{pmatrix} f_{17/3} & -f_4 & f_3 & f_{15/3} \\ -f_4 & f_{7/3} & -f_{4/3} & -f_{10/3} \\ f_3 & -f_{4/3} & f_{1/3} & f_{7/3} \\ f_{15/3} & -f_{10/3} & f_{7/3} & f_{13/3} \end{pmatrix} \quad (4 \text{ parameters}) \quad (4.19b)$$

$$E_{ij} = \begin{pmatrix} f_{17/3} & -f_4 & f_3 & f_{15/3} & f_{14/3} \\ -f_4 & f_{7/3} & -f_{4/3} & -f_{10/3} & -f_3 \\ f_3 & -f_{4/3} & f_{1/3} & f_{7/3} & f_2 \\ f_{15/3} & -f_{10/3} & f_{7/3} & f_{13/3} & f_4 \\ f_{14/3} & -f_3 & f_2 & f_4 & f_{11/3} \end{pmatrix} \quad (5 \text{ parameters}). \quad (4.19c)$$

The indices  $i, j$  range on the parameters  $\eta, \varphi_c, t_c, \lambda, \gamma$  in that order (we have  $F_{ij}E_{jk} = \delta_{ik}$ ). Finally, we need to compute the quantities  $\mathcal{D}_{00}$  and  $\mathcal{D}_{0i}$  entering the expression (4.13). These quantities are given with the required precision by (4.4)–(4.6). They are readily evaluated with the help of (4.14) and (4.17), and we find

$$\mathcal{D}_{00} = \frac{4G^2}{c^6} \frac{\rho_0^2}{f_{7/3}} h_{1/3} \quad (4.20a)$$

$$\mathcal{D}_{0i} = \frac{2G}{c^3} \frac{\rho_0^2}{f_{7/3}} G_i \quad (4.20b)$$

where we have, respectively for 3, 4 and 5 parameters,

$$G_i = \begin{pmatrix} g_3 \\ -g_{4/3} \\ g_{1/3} \end{pmatrix}, \quad \begin{pmatrix} g_3 \\ -g_{4/3} \\ g_{1/3} \\ g_{7/3} \end{pmatrix}, \quad \begin{pmatrix} g_3 \\ -g_{4/3} \\ g_{1/3} \\ g_{7/3} \\ g_2 \end{pmatrix}. \quad (4.20c)$$

In these expressions, the new moments  $g_\alpha$  and  $h_\alpha$  are defined by

$$g_\alpha = \int_0^{+\infty} \frac{d\omega \omega^{-\alpha}}{S_h(\omega)} \ln(\omega/\omega_s) \quad h_\alpha = \int_0^{+\infty} \frac{d\omega \omega^{-\alpha}}{S_h(\omega)} \ln^2(\omega/\omega_s). \quad (4.21)$$

By inserting (4.20) and (4.18) into the expression (4.13) of the variance  $\sigma_M^2$ , we then obtain our looked-for formula

$$\sigma_M^2 = \frac{c^6}{4G^2} \frac{f_{7/3}}{\rho_0^2} \frac{1}{h_{1/3} - F_{ij}G_iG_j} \quad (4.22)$$

(where we sum on repeated indices in  $F_{ij}G_iG_j$ ). As a check of the correctness of this formula, we can show that  $\sigma_M^2$  is independent of the particular choice of radiative coordinate

system we have made in (2.8), i.e. is independent of the value of the frequency  $\omega_s$ . From (4.16) and (4.21), we have  $\partial h_\alpha / \partial \omega_s = -2g_\alpha / \omega_s$  and  $\partial g_\alpha / \partial \omega_s = -f_\alpha / \omega_s$ , from which we deduce  $\partial [h_{1/3} - F_{ij} G_i G_j] / \partial \omega_s = 0$ . Thus, we have  $\partial (\sigma_M^2) / \partial \omega_s = 0$ .

The variance  $\sigma_M^2$  obtained in (4.22) is valid for any spectral density of noise  $S_h(\omega)$ . In order to compute it, we use some simplified models of noise in the detector. First we suppose that  $S_h(\omega)$  is infinite below the seismic cut-off  $\omega_s$ , and above some upper cut-off  $\omega_u$ ,

$$S_h(\omega) = \infty \quad \omega < \omega_s \quad \text{or} \quad \omega > \omega_u. \quad (4.23)$$

Then we choose, within the bandwidth  $[\omega_s, \omega_u]$ , either a model of white noise, i.e.

$$S_h(\omega) = S \quad \omega_s \leq \omega \leq \omega_u \quad (4.24)$$

where  $S$  is some constant, or a model of 'coloured' noise appropriate for shot noise in laser interferometric detectors that employ Fabry-Perot cavities and use standard recycling, i.e.

$$S_h(\omega) = K \omega_k \left[ 1 + \left( \frac{\omega}{\omega_k} \right)^2 \right] \quad \omega_s \leq \omega \leq \omega_u \quad (4.25a)$$

(see, for example, [1]). The constant  $K$  in (4.25a) depends notably on the laser power and on the reflectivities of the end mirrors. (We shall not need the expression of  $K$  nor the value of  $S$ .) The frequency  $\omega_k$  in (4.25a) is the so-called 'knee' frequency, and can be chosen by the experimenters at will. We adopt here the value of  $\omega_k$  that maximizes (all other parameters remaining fixed) the SNR (4.15), i.e. that maximizes the moment  $f_{7/3}$ . This value is known [41] to be

$$\omega_k = 1.44 \omega_s. \quad (4.25b)$$

The relevant moments  $f_\alpha$ ,  $g_\alpha$  and  $h_\alpha$  are computed using the two models of noise (4.24) and (4.25), and substituted into (4.22). It is immediately seen that the standard deviation  $\sigma_M$  will take the form

$$\sigma_M = a \frac{c^3}{G \rho_0 \omega_s} \quad (4.26)$$

where  $a$  is a pure dimensionless number, depending only on the type of noise in the detector (white or coloured) and on the ratio  $\omega_u / \omega_s$ . The number  $a$  is composed of many residual dimensionless integrals resulting from the various moments  $f_\alpha$ ,  $g_\alpha$  and  $h_\alpha$ . We have computed its numerical value in the case  $\omega_u / \omega_s = 20$  (for instance  $\omega_s / 2\pi = 100$  Hz and  $\omega_u / 2\pi = 2000$  Hz as will be used in the simulations of section 5), and obtain

$$a = 0.84, 2.21, 8.46 \quad (\text{white noise; resp. 3, 4, 5 parameters}) \quad (4.27a)$$

$$a = 2.40, 6.46, 24.26 \quad (\text{coloured noise; resp. 3, 4, 5 parameters}). \quad (4.27b)$$

The standard deviation  $\sigma_M$  as given by (4.26) is inversely proportional to the SNR, and also inversely proportional to the lower cut-off  $\omega_s$ . Note that when we improve the detection by lowering  $\omega_s$ , the standard deviation  $\sigma_M$  decreases, contrary to what could be expected from (4.26), and thus the measurement of  $M$  becomes more precise. This is of course due to the fact that the SNR  $\rho_0$  also depends on  $\omega_s$ . For instance, in the case of an inspiralling

binary and of the model of noise (4.25) (with fixed ratio  $\omega_u/\omega_s$ ),  $\rho_0$  depends on  $\omega_s$  like  $\omega_s^{-7/6}$  and so  $\rho_0\omega_s$  varies like  $\omega_s^{-1/6}$  which increases when  $\omega_s$  decreases.

For a high enough value of the SNR, the precision  $\sigma_M$  in the measurement of  $M$  becomes smaller than the value of  $M$  itself. When this occurs, we are able to attribute to the total mass  $M$  a definite non-zero value at the one-sigma confidence level, and we are able to detect the presence of  $\theta(\omega)$  in the signal. Thus, we adopt the condition  $\sigma_M \leq M$  as a criterion to decide that  $\theta(\omega)$  is detected (at the one- $\sigma$  level). By (4.26) this condition reads as

$$\rho_0 \geq a \frac{c^3}{GM\omega_s}. \quad (4.28)$$

Note that (4.28) can be fulfilled for reasons owing both to the source and to the detector. For instance, it can be true because the mass of the source is very large or because the source is located very near. It can also be true because the seismic cut-off of the detector is very low. In the case of an inspiralling binary made of two neutron stars with total mass  $2.8M_\odot$ , with  $\omega_s = 2\pi \times 100$  Hz and the numerical values (4.27) of  $a$ , we obtain

$$\rho_0 \geq 97, 254, 973 \quad (\text{white noise; resp. 3, 4, 5 parameters}) \quad (4.29a)$$

$$\rho_0 \geq 276, 743, 2790 \quad (\text{coloured noise; resp. 3, 4, 5 parameters}). \quad (4.29b)$$

In the case of a black-hole binary with total mass  $20M_\odot$ , we obtain

$$\rho_0 \geq 13, 36, 136 \quad (\text{white noise; resp. 3, 4, 5 parameters}) \quad (4.30a)$$

$$\rho_0 \geq 39, 104, 390 \quad (\text{coloured noise; resp. 3, 4, 5 parameters}). \quad (4.30b)$$

Note that the SNR  $\rho_0$  in (4.28)–(4.30) can equally well be replaced by the optimal SNR  $\rho$ ; see (A.11) in the appendix.

The prospects, opened by the estimates (4.29) and (4.30), of detecting the phase modulation  $\theta(\omega)$  have been discussed in the introduction. We now turn to a numerical simulation of the detection of the tail contribution in a real experiment. For simplicity, we consider only the case of three independent parameters in the wavefront. This corresponds to the case for which we know *a priori* that the spins of the stars are negligible and, for instance, that the two masses are nearly equal.

## 5. Numerical investigation of the detection of the tail contribution

### 5.1. Construction of a lattice of filters

The question of the construction of a lattice of matched filters (or ‘templates’) for the detection of  $\theta(\omega)$  needs to be settled before the simulation. The templates are given by (3.11), i.e.

$$\tilde{q}(\omega; \iota\lambda_\alpha) = \gamma' \frac{\tilde{k}(\omega; \iota\lambda_\alpha)}{S_h(\omega)}. \quad (5.1)$$

They depend on a set of test parameters  $\iota\lambda_\alpha$ , where the label  $\alpha$  ranges from 0 to  $N$ , which are assumed to be all independent of each other. Following [43, 44], we choose the arbitrary

constant  $\gamma'$  in (5.1) to be such that the noise power of the filtered output of the detector is unity, i.e.

$$\int_{-\infty}^{\infty} \frac{d\omega}{2\pi} S_h(\omega) |\tilde{q}(\omega; \iota\lambda)|^2 = 1 \implies \gamma' = \langle k(\iota\lambda), k(\iota\lambda) \rangle^{-1/2}. \quad (5.2)$$

With this choice of normalization, we can write the family of filters (5.1) in the form

$$\tilde{q}(\omega; \iota\lambda_\alpha) = \frac{\tilde{u}(\omega; \iota\lambda_\alpha)}{S_h(\omega)} \quad (5.3)$$

where  $\tilde{u}(\omega; \iota\lambda_\alpha)$  denotes a family of signals of unit SNR (3.8) or, using the terminology of [43, 44], of unit strength, i.e.

$$\tilde{u}(\omega; \iota\lambda) = \frac{\tilde{k}(\omega; \iota\lambda)}{\langle k(\iota\lambda), k(\iota\lambda) \rangle^{1/2}} \implies \langle u(\iota\lambda), u(\iota\lambda) \rangle = 1. \quad (5.4)$$

Let us first note that, in practice, it is impossible to use the family of filters (5.1) or (5.3) in which the test parameters  $\iota\lambda_\alpha$  take on all possible values. Thus, one must consider only a finite (discrete) lattice of filters. Since it is unlikely that any member of the family will have its parameters exactly matching those of a signal present in the data train, we will not reach, in general, the optimal SNR (3.8). We denote by  $\kappa$  the maximal relative drop ( $\kappa > 1$ ) in the optimal SNR that is due to the discrete nature of the lattice of filters. Thus, if  $\rho$  is the optimal SNR, we assume that  $\kappa^{-1}\rho$  is the *smallest* SNR obtained by filtering an arbitrary signal through the discrete lattice of filters. In an on-line analysis of data, a compromise is clearly in order. On one hand, we want to minimize  $\kappa$  in order to reach as high a SNR as possible, and on the other hand we want to minimize the number of filters in the lattice (and thus to increase  $\kappa$ ) in order to save on computing time. Here, the problem is simpler because our analysis will not be on-line, but rather will be a further analysis later (see the appendix). Thus, we shall not optimize the value of  $\kappa$ , but simply calculate the spacing between filters, in all directions of the parameter space, for some good value of  $\kappa$ , say  $\kappa^{-1} = 0.99$ .

In order to decide upon the spacing between filters, we consider the behaviour of the correlation function

$$C(\lambda_\alpha, \iota\lambda_\alpha) = \langle u(\lambda_\alpha), u(\iota\lambda_\alpha) \rangle. \quad (5.5)$$

This correlation function is equal to (the value at  $t = 0$  of) the correlation between the filter (5.3), parametrized by test parameters  $\iota\lambda_\alpha$ , and a signal of unit strength  $\tilde{u}(\lambda_\alpha)$ , parametrized by signal parameters  $\lambda_\alpha$ . In the notation of (3.8) and (3.12), we have  $C(\lambda_\alpha, \iota\lambda_\alpha) = \sigma(\lambda_\alpha, \iota\lambda_\alpha) / \rho(\lambda_\alpha)$ , where the dependence on the signal parameters  $\lambda_\alpha$  is explicitly indicated. By the matched filtering theorem, the correlation (5.5) attains its maximum *one* when all the test parameters exactly match those of the signal,  $\iota\lambda_\alpha = \lambda_\alpha$ . Looking for the spacing between filters in the particular direction  $\xi = \lambda_{\alpha_0}$  (where  $0 \leq \alpha_0 \leq N$ ) of the parameter space, we maximize (5.5) over all the test parameters except  $\iota\xi = \iota\lambda_{\alpha_0}$ . That is, we consider the maximum correlation

$$C_{\max}(\xi, \iota\xi) = \max_{\substack{\iota\lambda_\alpha \\ \alpha \neq \alpha_0}} C(\lambda_\alpha, \iota\lambda_\alpha) \quad (5.6)$$

as a function of the mismatch between  $\xi$  and  ${}_{\iota}\xi$  [43, 44] (*a priori*,  $C_{\max}$  still depends on the other signal parameters  $\lambda_{\alpha}$ ,  $\alpha \neq \alpha_0$ , but we do not mention this for simplicity). Note that, due to the existence of covariance amongst the various parameters, the maximum correlation (5.6) does *not* reach its maximum when the test parameters  ${}_{\iota}\lambda_{\alpha}$ ,  $\alpha \neq \alpha_0$ , are equal to the signal parameters  $\lambda_{\alpha}$ ,  $\alpha \neq \alpha_0$ . Indeed, the mismatch between  $\xi$  and  ${}_{\iota}\xi$  induces in (5.6) a mismatch on the other parameters as well.

Let  $[\xi_L, \xi_U]$  be an interval over which the test parameters  ${}_{\iota}\xi$  are chosen. This interval represents for instance an astrophysically interesting range of values of  $\xi$ , or an interval surrounding some preliminary measured value  ${}_m\xi^{(0)}$  obtained in an on-line analysis of data. We denote by  $\xi_k$  the  $k$ th value of the test parameter  ${}_{\iota}\xi$  in the lattice of filters, some values of the other parameters  ${}_{\iota}\lambda_{\alpha}$ ,  $\alpha \neq \alpha_0$ , being given. We begin at the lower end of the interval by choosing a filter with  $\xi_1 = \xi_L$ . Then, following [43, 44], we construct the  $(k+1)$ th filter  $\xi_{k+1}$  from the  $k$ th filter  $\xi_k$  (with  $\xi_{k+1} > \xi_k$ ) by defining the spacing between  $\xi_k$  and  $\xi_{k+1}$  to be

$$\Delta\xi_{k,k+1} := \xi_{k+1} - \xi_k = \Delta_+\xi_k + \Delta_-\xi_{k+1} \quad (5.7)$$

where  $\Delta_+\xi_k$  and  $\Delta_-\xi_{k+1}$  are the increment from  $\xi_k$  and decrement from  $\xi_{k+1}$  at which the optimal SNR  $\rho$  drops to the value  $\kappa^{-1}\rho$ , respectively. That is,  $\Delta_+\xi_k$  and  $\Delta_-\xi_{k+1}$  are such that

$$C_{\max}(\xi_k + \Delta_+\xi_k, \xi_k) = C_{\max}(\xi_{k+1} - \Delta_-\xi_{k+1}, \xi_{k+1}) = \kappa^{-1}. \quad (5.8)$$

The construction terminates at the  $n$ th filter such that  $\xi_n < \xi_U < \xi_n + \Delta_+\xi_n$ . The lattice of filters so constructed is such that the  $k$ th filter yields a SNR larger than  $\kappa^{-1}\rho$  for all signals having  $\xi \in [\xi_k - \Delta_-\xi_k, \xi_k + \Delta_+\xi_k]$ .

We now consider specifically the waveform (2.15) with (4.14). This waveform depends on four parameters (besides the amplitude parameter  $\mathcal{A}$ ): three ‘Newtonian’ parameters  $\lambda_i = \{\eta, \varphi_c, t_c\}$ , and the total mass  $M$  which is in front of the tail contribution. For the purpose of the simulation, it is convenient to use, instead of the parameter  $\eta$ , the time  $\tau$  left until coalescence starting from the ‘arrival’ time  $t_s$  at which the frequency reaches the seismic cut-off  $\omega_s$ . We have  $\tau = (5\eta/3)\omega_s^{-8/3}$ . It is also convenient to use, instead of  $t_c$  and  $\varphi_c$ , the arrival time  $t_s = t_c - \tau$  and the initial phase  $\varphi_s$  of the signal at  $t_s$ . We discuss each of these parameters separately.

*The coalescing time  $\tau$ .* Figure 1 shows the behaviour of the correlation function  $C_{\max}(\tau, {}_{\iota}\tau)$  defined in (5.6), as a function of the mismatch  ${}_{\iota}\tau - \tau$ . The function is a monotonically decreasing function of  $|{}_{\iota}\tau - \tau|$  taking its maximum 1 when  ${}_{\iota}\tau = \tau$ , and which is symmetric about the vertical axis because, in a signal of unit strength, the parameter  $\tau$  arises only linearly in the phase of the signal [43, 44].  $C_{\max}(\tau, {}_{\iota}\tau)$  is plotted for both the white noise and the coloured noise defined in (4.24) and (4.25). The curves fall off much more steeply when the detector noise is white than when it is coloured. This is to be expected because the detector is relatively narrowband in the coloured noise case as compared to the white noise case. Since the curves depend solely, for a given type of noise, on the difference  ${}_{\iota}\tau - \tau$ , apart from a slight dependence on the total mass  $M$ , we can choose the distance (5.7) between filters to be a constant  $\Delta\tau$ . From figure 1, we see that  $\Delta\tau = 1$  ms is sufficient to ensure in any case a value of  $\kappa^{-1}$  better than 0.99.

*The total mass  $M$ .* The function  $C_{\max}(M, {}_{\iota}M)$ , shown in figure 2, exhibits the same behaviour as in figure 1 for similar reasons. With  $\kappa^{-1} = 0.99$ , we see that the distance between filters should be approximately  $\Delta M = 80M_{\odot}$  in the white noise case and much

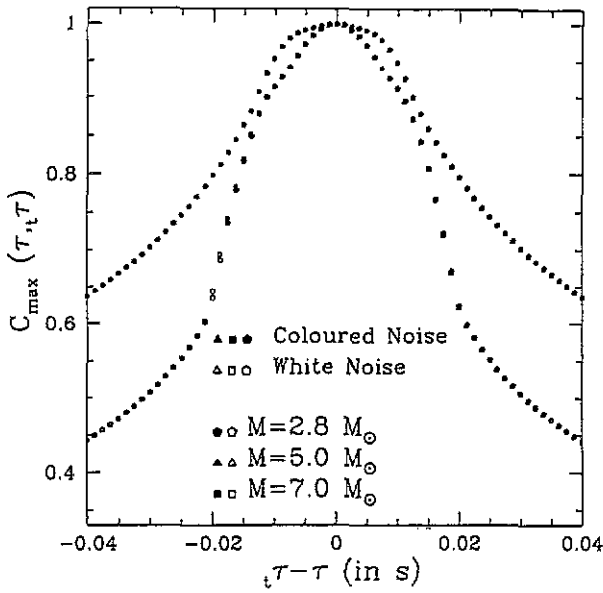


Figure 1. The correlation function  $C_{\max}(\tau, \tau)$  plotted against  $t\tau - \tau$ .

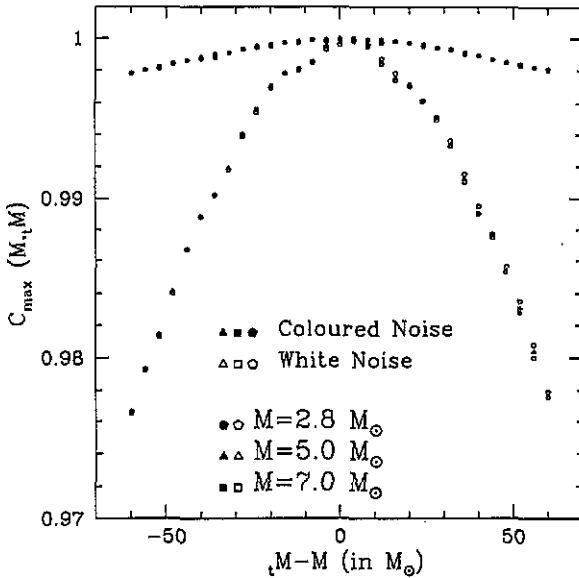


Figure 2. The correlation function  $C_{\max}(M, M)$  plotted against  $tM - M$ .

larger in the coloured noise case. Thus, very few filters are needed in the  $M$ -direction of the parameter space to ensure a good value of  $\kappa^{-1}$ . This, of course, reflects the fact that  $\theta(\omega)$  is a sub-dominant effect of very small post-Newtonian order. Thus, the number of filters in the  $M$ -direction will be determined only by the precision at which one wants to measure  $M$ .

*The time of arrival  $t_s$ .* The unknown time of arrival of the signal is characterized by the lag  $j$  of the filter relative to the output of the detector in the discrete correlation (5.9) below. The number of filters for the time of arrival is determined by the sampling rate  $\Delta^{-1}$  at which output and filters are sampled.  $\Delta^{-1}$  has to be larger than twice the bandwidth. The precision in the arrival time of the signal is limited to  $\Delta$ .

The initial phase  $\varphi_s$ . We need only two filters in the  $\varphi_s$ -direction of the parameter space, for instance, one corresponding to  ${}_t\varphi_s = 0$  and one corresponding to  ${}_t\varphi_s = \pi/2$  (see, for example, [48, 43]).

## 5.2. Numerical simulation

The waveform  $h(t)$  of an inspiralling binary, composed of the wavefront (4.14) and of the tail contribution  $\theta(\omega)$ , is added to simulated Gaussian noise  $n(t)$ . The parameters of the waveform are  $\mathcal{A}$ ,  $M$ ,  $\tau$ ,  $\varphi_s$ ,  $t_s$ . The noise is chosen to be either white or coloured (see (4.24) and (4.25)). The data  $o(t) = h(t) + n(t)$  is our simulated noisy detector output. It is filtered through a family of templates  $q(t)$  constructed using the algorithm developed above.

For numerical implementation of the filtering process we need to consider the discrete version of the correlation (3.5) between the detector output  $o(t)$  and a filter  $q(t)$  satisfying the normalization condition (5.2). Let  $o_k$  and  $q_k$ , with  $k = 0, \dots, K-1$ , be the  $K$  samples of the detector output and filter, respectively, sampled at the rate  $\Delta$ :  $o_k \equiv o(t_k)$ ,  $q_k \equiv q(t_k)$  and  $t_k = k\Delta$ . The discrete correlation  $\sigma_j \equiv \sigma(t_j)$  of the samples  $o_k$  and  $q_k$  is then given by

$$\frac{\sigma_j}{\Delta} = \sum_{k=0}^{K-1} o_k q_{k+j} = \frac{1}{K} \sum_{l=0}^{K-1} \tilde{o}_l \tilde{q}_l^* e^{i2\pi lj/K} \quad (5.9)$$

where  $j$  is the lag, where  $\tilde{o}_l = \sum_{k=0}^{K-1} o_k \exp(i2\pi lk/K)$  and  $\tilde{q}_l = \sum_{k=0}^{K-1} q_k \exp(i2\pi lk/K)$  are the discrete Fourier coefficients of the detector output and filter, and where the second equality follows from the discrete correlation theorem. Due to the availability of fast Fourier transforms it is numerically less expensive to compute the correlation in the Fourier domain (second equality in (5.9)). Note that the use of the discrete correlation (5.9) implicitly assumes that the filter  $q_k$  is periodic with period  $K$ , i.e.  $q_{k+K} = q_k$ . This periodicity introduces spurious contributions in the correlation, and we solve this problem by ‘padding’ the filter with zeros so that the correct correlation is nevertheless obtained for some subset of values of the lag (see [48]).

The family of templates we use in the simulation has the following characteristics. The bandwidth is 100–2000 Hz and the sampling rate is  $\Delta^{-1} = 4000$  Hz. The range of values of  ${}_t\tau$  is  $[\tau - 0.01 \text{ s}, \tau + 0.01 \text{ s}]$ , and the distance between filters is  $\Delta\tau = 1$  ms. We use a rather small range of values of  ${}_t\tau$  because it is assumed that an approximate value of  $\tau$  is already known from a preliminary data analysis. However, this range is large enough to take care of the covariance between  $\tau$  and the other parameters (notably  $M$ ). The range of values of  ${}_tM$  is chosen to be very large ( $\sim 100M_\odot$ ) and some negative values of  ${}_tM$  are tried. The distance between filters  $\Delta M$  is adjusted so that it is smaller than the precision in the measurement of  $M$ . Thus, in the computation below, the precision  $\sigma_M$  is meaningful only as long as  $\Delta M < \sigma_M$ . If a computation yields a value of  $\sigma_M$  smaller than  $\Delta M$ , we have to redo the computation with a finer lattice of filters.

By maximizing the correlation (5.9) over the family of templates, for a given realization of noise, we obtain a first set of measured parameters. The same signal is then added to a different realization of noise and the resultant data is again filtered through the same family of templates, giving us another set of measured parameters. The whole procedure is repeated for a large number of realizations of noise ( $\sim 50$ ). The averages of the distribution of the measured parameters, together with the standard deviations around the averages, are then computed. This yields notably the standard deviation  $\sigma_M$  of the measured total mass. (By a slight abuse of the notation, we denote by the same symbol  $\sigma_M$  as in sections 3 and 4 what corresponds here only to a *finite* number of realizations of noise.) The results of the

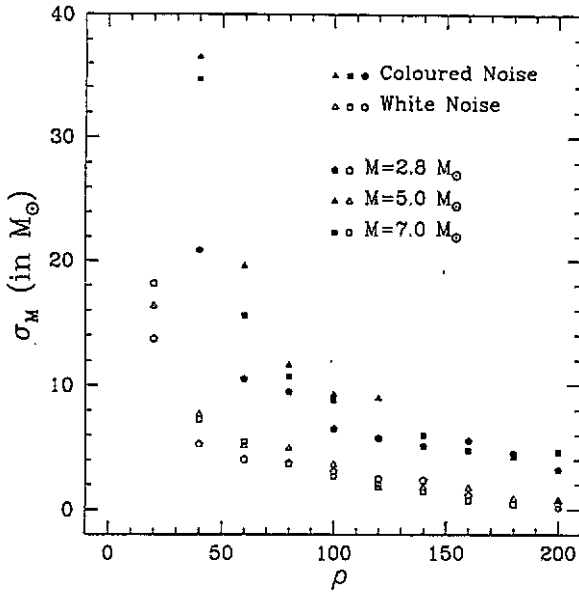


Figure 3. The standard deviation  $\sigma_M$  in the measurement of  $M$  plotted against the optimal SNR  $\rho$ .

computation of  $\sigma_M$  are shown in figure 3, where this quantity is plotted against the optimal SNR (3.8) of the signal, for various values of the total mass  $M$  of the signal, and for both the white and coloured noises.

Based on figure 3 we can conclude the following. (i) The standard deviation  $\sigma_M$  is a decreasing function of the SNR which depends on the type of noise and is only slightly sensitive on the total mass  $M$  of the signal. This behaviour is in rather good agreement with the theoretical result (4.26) (which we recall was computed in the idealized cases of high SNR and of an infinite number of noise realizations). (ii) The value of  $\sigma_M$  is significantly higher in the coloured noise case than in the white noise case. This is to be expected for the same reason as noticed earlier: the detector is relatively narrowband in the former case as compared to the latter case, and thus the precision on the measurement of  $M$  is lower. (iii) We see that in order to detect the phase  $\theta(\omega)$  at the one-sigma level (i.e. to have  $\sigma_M \leq M$ ) in the case of a binary with total mass  $M = 2.8M_\odot$ , we need a SNR larger than 200 with coloured noise, and equal to about 100 with white noise. If the total mass is  $M = 20M_\odot$ , the minimal SNR is about 50 with coloured noise and about 15 with white noise. These numerical values are in agreement with the analytical computations (see (4.29) and (4.30) for three independent parameters in the wavefront).

### Acknowledgments

It is a pleasure to thank Curt Cutler and Eanna Flanagan for important comments, and the members of the VIRGO experiment at Orsay for discussions. One of us (BSS) would like to thank Thibault Damour for invitation at the Observatoire de Paris–Meudon.

### Appendix. A non-optimal filtering

The aim of this appendix is to investigate the consequences of using a family of filters matched on  $\tilde{H}_0(\omega)$  instead of the real wave  $\tilde{h}(\omega)$  including  $\theta(\omega)$ . That is, we assume that

the experimenters correlate the output of the detector (3.1) not with the optimal family of filters (3.11), but with the non-optimal family of filters

$$\tilde{q}_0(\omega; {}_t\lambda_i) = \gamma' \frac{\tilde{K}_0(\omega; {}_t\lambda_i)}{S_h(\omega)} \quad (\text{A.1})$$

where  $\tilde{K}_0$  is defined in (4.2), and where  ${}_t\lambda_i$  is a family of test parameters of the wavefront, the Latin index ranging from  $i = 1$  to  $N$ . By substituting (A.1) into (3.5) and choosing  $t = 0$ , we obtain, instead of (3.12),

$$\sigma_0({}_t\lambda_i) = \frac{\langle o, K_0({}_t\lambda_i) \rangle}{\langle K_0({}_t\lambda_i), K_0({}_t\lambda_i) \rangle^{1/2}} \quad (\text{A.2})$$

The experimenters then choose as their best estimate of the parameters of the source the measured values  ${}_m\lambda_i^{(0)}$  that maximize the ratio (A.2), i.e. such that

$$\frac{\partial \sigma_0}{\partial {}_t\lambda_i} ({}_m\lambda_i^{(0)}) = 0 \quad i = 1, 2, \dots, N. \quad (\text{A.3})$$

We denote the difference between the source parameters and the non-optimally measured ones by

$$\delta\lambda_i^{(0)} = \lambda_i - {}_m\lambda_i^{(0)}. \quad (\text{A.4})$$

The expression of  $\delta\lambda_i^{(0)}$  can be immediately deduced, in the high SNR approximation, from (3.15) by simple replacement of  $h$  by  $H_0$  and of  $n$  by  $n + \delta h$ , where  $\delta h = h - H_0$  denotes the tail term. We obtain

$$\delta\lambda_i^{(0)} = C_{ij}^{(0)} \left\{ - \left\langle n + \delta h, \frac{\partial H_0}{\partial \lambda_j} \right\rangle + \frac{\langle n + \delta h, H_0 \rangle}{\langle H_0, H_0 \rangle} \left\langle H_0, \frac{\partial H_0}{\partial \lambda_j} \right\rangle \right\} \quad (\text{A.5})$$

where  $C_{ij}^{(0)}$  is the covariance matrix of the wavefront, inverse of the matrix (4.7). The matrix  $C_{ij}^{(0)}$  is given by (4.18) and (4.19) in the case of inspiralling binaries. As we see from (A.5), the variables  $\delta\lambda_i^{(0)}$  are Gaussian (for Gaussian noise). But, contrarily to the variables  $\delta\lambda_\alpha = \{\delta M, \delta\lambda_i\}$  associated with the optimal filtering of section 3, their expectation values are not zero but given by

$$\overline{\delta\lambda_i^{(0)}} = C_{ij}^{(0)} \left\{ - \left\langle \delta h, \frac{\partial H_0}{\partial \lambda_j} \right\rangle + \frac{\langle \delta h, H_0 \rangle}{\langle H_0, H_0 \rangle} \left\langle H_0, \frac{\partial H_0}{\partial \lambda_j} \right\rangle \right\}. \quad (\text{A.6})$$

As for their second-order moments, they are

$$\overline{(\delta\lambda_i^{(0)} - \overline{\delta\lambda_i^{(0)}})(\delta\lambda_j^{(0)} - \overline{\delta\lambda_j^{(0)}})} = C_{ij}^{(0)}. \quad (\text{A.7})$$

Equation (A.6) means that by using the non-optimal filtering (A.1) we make *errors* (on average) on the determination of the parameters (A.4). These errors are of course of the same order  $O(G) = O(\varepsilon^3)$  as the tail; they have explicitly in factor the total mass  $M$  of the

source. Using  $\delta h = M \partial h / \partial M$  and the expression (3.16) of the matrix  $\mathcal{D}_{\alpha\beta}$ , together with (4.10), we can express (A.6) in the simple form

$$\overline{\delta\lambda_i^{(0)}} = -M \mathcal{D}_{0j} C_{ij}^{(0)} = M \frac{C_{0i}}{C_{00}} \quad (\text{A.8})$$

(where higher-order terms are neglected). The errors (A.8) can be readily computed in the case of an inspiralling binary, where we have  $\lambda_i = \{\eta, \varphi_c, t_c\}$ . Inserting (4.18) and (4.20b) into (A.8) yields

$$\overline{\delta\lambda_i^{(0)}} = -\frac{2GM}{c^3} F_{ij} G_j. \quad (\text{A.9})$$

Finally, let us check that the maximal value  $\rho_0$  of the SNR obtained by means of the non-optimal filtering based on  $\tilde{H}_0$  is equal, modulo negligible higher-order  $O(G^2)$  terms (using the same notation as in (4.3) and (4.4)), to the optimal value  $\rho$  of the SNR obtained by means of the optimal filtering of section 3. Indeed, from (A.2) and (A.3), the non-optimal SNR is

$$\rho_0 = \overline{\sigma_0(\lambda_i^{(0)})} = \overline{\sigma_0(\lambda_i)} + O(G^2) = \frac{\langle h, H_0 \rangle}{\langle H_0, H_0 \rangle^{1/2}} + O(G^2). \quad (\text{A.10})$$

Inserting  $H_0 = h - \delta h$  with  $\delta h = O(G)$ , we then obtain

$$\rho_0 = \langle h, h \rangle^{1/2} + O(G^2) = \rho + O(G^2) \quad (\text{A.11})$$

where  $\rho$  denotes the optimal SNR (3.8). Thus, it is not possible to detect the phase  $\theta(\omega)$  by simply comparing the values of the SNRs obtained by means of the optimal filtering of section 3 and of the non-optimal filtering of this appendix. *A contrario*, this means that it is not necessary to include this effect in the filters of a preliminary on-line analysis of data aiming at *searching* for the signal.

## References

- [1] Thorne K S 1987 *300 Years of Gravitation* ed S W Hawking and W Israel (Cambridge: Cambridge University Press)
- [2] Schutz B F 1989 *Class. Quantum Grav.* **6** 1761
- [3] Clark J P A, van den Heuvel E P J and Sutantyo W 1979 *Astron. Astrophys.* **72** 120
- [4] Phinney E S 1991 *Astrophys. J.* **380** L17
- [5] Narayan R, Piran T and Shemi A 1991 *Astrophys. J.* **379** L17
- [6] Bradaschia C *et al* 1991 *Proc. Banff Summer Inst. on Gravitation (Banff, 1990)* ed R Mann and P Wesson (Singapore: World Scientific)
- [7] Abramovici A *et al* 1992 *Science* **256** 325
- [8] Krolak A, Lobo J A and Meers B J 1991 *Phys. Rev. D* **43** 2470
- [9] Finn L S and Chernoff D F 1993 *Phys. Rev. D* **47** 2198
- [10] Cutler C, Apostolatos T A, Bildsten L, Finn L S, Flanagan E E, Kennefick D, Markovic D M, Ori A, Poisson E, Sussman G J and Thorne K S 1993 *Phys. Rev. Lett.* **70** 2984
- [11] Blanchet L and Schäfer G 1993 *Class. Quantum Grav.* **10** 2699
- [12] Bonnor W B and Rotenberg M A 1966 *Proc. R. Soc. A* **289** 247
- [13] Couch W E, Torrence R J, Janis A I and Newman E T 1968 *J. Math. Phys.* **9** 484
- [14] Hunter A J and Rotenberg M A 1969 *J. Phys. A: Math. Gen.* **2** 34
- [15] Bonnor W B 1974 *Ondes et Radiations Gravitationnelles* (Paris: CNRS) p 73
- [16] Thorne K S and Kovács S J 1975 *Astrophys. J.* **200** 245

- [17] Thorne K S 1980 *Rev. Mod. Phys.* **52** 299
- [18] Blanchet L Contribution à l'étude du rayonnement gravitationnel émis par un système isolé *Thèse d'habilitation* Université P et M Curie p 195 (unpublished)
- [19] Schäfer G 1990 *Astron. Nachr.* **311** 213
- [20] Peters P C 1966 *Phys. Rev.* **146** 938
- [21] Kundt W and Newman E T 1968 *J. Math. Phys.* **9** 2193
- [22] McLenaghan R G 1969 *Proc. Camb. Phil. Soc.* **65** 139
- [23] Price R H 1972 *Phys. Rev. D* **5** 2419
- [24] Price R H 1972 *Phys. Rev. D* **5** 2439
- [25] Bardeen J M and Press W H 1973 *J. Math. Phys.* **14** 7
- [26] Schmidt B G and Stewart J M 1979 *Proc. R. Soc. A* **367** 503
- [27] Porrill J and Stewart J M 1981 *Proc. R. Soc. A* **376** 451
- [28] Leaver E W 1986 *Phys. Rev.* **34** 384
- [29] Fourès-Bruhat Y 1952 *Acta Math.* **88** 141
- [30] Bertotti B and Plebanski J 1960 *Ann. Phys., NY* **11** 169
- [31] Bruhat Y 1964 *Ann. Mat. Pure Appl.* **64** 191
- [32] Friedlander F G 1975 *The Wave Equation on a Curved Spacetime* (Cambridge: Cambridge University Press)
- [33] Waylen P C 1978 *Proc. R. Soc. A* **362** 233
- [34] Choquet-Bruhat Y, Christodoulou D and Francaviglia M 1979 *Ann. Inst. Henri Poincaré A* **31** 399
- [35] Carminati J and McLenaghan R G 1986 *Ann. Inst. Henri Poincaré (Physique Théorique)* **A 44** 115
- [36] Blanchet L and Damour T 1992 *Phys. Rev. D* **46** 4304
- [37] Blanchet L and Damour T 1988 *Phys. Rev. D* **37** 1410
- [38] Blanchet L 1993 *Phys. Rev. D* **47** 4392
- [39] Poisson E 1993 *Phys. Rev. D* **47** 1497
- [40] Wiseman A G 1993 *Phys. Rev. D* **48** 4757
- [41] Krolak A 1989 *Gravitational Wave Data Analysis* ed B F Schutz (Dortrecht: Kluwer)
- [42] Blanchet L and Sathyaprakash B S 1994 *Phys. Rev. Lett.* submitted
- [43] Sathyaprakash B S and Dhurandhar S V 1991 *Phys. Rev. D* **44** 3819
- [44] Dhurandhar S V and Sathyaprakash B S 1993 *Phys. Rev. D* **49** 1707
- [45] Wainstein L A and Zubakov L D 1962 *Extraction of Signals from Noise* (Englewood, NJ: Prentice-Hall)
- [46] Blanchet L and Damour T 1989 *Ann. Inst. H. Poincaré (Physique Théorique)* **50** 377
- [47] Damour T and Iyer B R 1991 *Ann. Inst. H. Poincaré (Physique Théorique)* **54** 115
- [48] Schutz B F 1989 *The Detection of Gravitational Radiation* ed D Blair (Cambridge: Cambridge University Press)
- [49] Davis M H A 1989 *Gravitational Wave Data Analysis* ed B F Schutz (Dortrecht: Kluwer)
- [50] Finn L S 1993 *Phys. Rev. D* **46** 5236
- [51] Kidder L E, Will C M and Wiseman A G 1993 *Phys. Rev. D* **47** R4183
- [52] Cutler C and Flanagan E 1994 *Phys. Rev. D* **49** 2658
- [53] Flanagan E 1994 Private communication

